Published in final edited form as:
Nat Genet. 2011 May ; 43(5): 442–446. doi:10.1038/ng.810.

Exome sequencing identifies GRIN2A as frequently mutated in melanoma

Xiaomu Wei[1], **Vijay Walia**[1,12], **Jimmy C Lin**[2,12], **Jamie K Teer**[3], **Todd D Prickett**[1], **Jared Gartner**[1], **Sean Davis**[4], **NISC Comparative Sequencing Program**[5], **Katherine Stemke-Hale**[6], **Michael A Davies**[6,7], **Jeffrey E Gershenwald**[8,9], **William Robinson**[10], **Steven Robinson**[10], **Steven A Rosenberg**[11], and **Yardena Samuels**[1]

[1]The Cancer Genetics Branch, National Human Genome Research Institute, National Institutes of Health (NIH), Bethesda, Maryland, USA.

[2]Ludwig Center for Cancer Genetics and Therapeutics and Howard Hughes Medical Institute at the Johns Hopkins Kimmel Cancer Center, Baltimore, Maryland, USA.

[3]Genetic Disease Research Branch, National Human Genome Research Institute, NIH, Bethesda, Maryland, USA.

[4]The Genetics Branch, National Cancer Institute, NIH, Bethesda, Maryland, USA.

[5]NIH Intramural Sequencing Center, National Human Genome Research Institute, NIH, Bethesda, Maryland, USA.

[6]Department of Systems Biology, The University of Texas MD Anderson Cancer Center, Houston, Texas, USA.

[7]Department of Melanoma Medical Oncology, The University of Texas MD Anderson Cancer Center, Houston, Texas, USA.

[8]Department of Surgical Oncology, The University of Texas MD Anderson Cancer Center, Houston, Texas, USA.

[9]Department of Cancer Biology, The University of Texas MD Anderson Cancer Center, Houston, Texas, USA.

Correspondence should be addressed to Y.S. (samuelsy@mail.nih.gov)..
[12]These authors contributed equally to this work.

AUTHOR CONTRIBUTIONS
X.W., V.W., J.C.L., J.K.T., T.D.P. and Y.S. designed the study; K.S.-H., M.A.D., J.E.G., W.R., S.R. and S.A.R. collected and analyzed the melanoma samples; X.W., J.K.T., J.G., J.C.L., S.D. and the NISC Comparative Sequencing Program analyzed the genetic data; V.W. and T.D.P. performed and analyzed the functional data. All authors contributed to the final version of the paper.

URLs. Green Group (cross_match), http://www.phrap.org; Laboratory of Thomas Ried, http://www.riedlab.nci.nih.gov; bam2mpg, http://research.nhgri.nih.gov/software/bam2mpg/; 1000 Genomes Project 11_2010 data release project, ftp://ftp-trace.ncbi.nih.gov/1000genomes/ftp/release/20100804/; Gene Ontology, http://www.geneontology.org/; Kyoto Encyclopedia of Genes and Genomes, http://www.genome.jp/kegg; MSigDB, http://www.broadinstitute.org/gsea/msigdb; R, http://www.r-project.org.

Accession codes. Data from this study are deposited in dbSNP. Accession codes: *BRAF*, CCDS5863.1; *CPT1A*, CCDS8185.1; *DCC*, CCDS11952.1; *FCRL1*, CCDS1170.1; *LRRN3*, CCDS5754.1; *NOS1*, CCDS41842.1; *PLCH1*, CCDS33881.1; *SLC17A5*, CCDS4981.1; *TRRAP*, CCDS5659.1; *ZNF831*, CCDS42894.1; *GRIN2A*, CCDS10539.1; *CCDC63*, CCDS9151.1; *TMEM132B*, CCDS41859.1; *PLCB4*, CCDS13104.1; *AKR1B10*, CCDS5832.1; *TAS2R60*, CCDS5885.1; *KHDRBS2*, CCDS4963.1; *PTPRO*, CCDS8675.1; *SYT4*, CCDS11922.1; *UGT2B10*, NM_001075.4; *SLC6A11*, CCDS2602.1; *C12orf63*, CCDS9062.1; *PCDHB8*, CCDS4250.1.

Note: Supplementary information is available on the Nature Genetics website.

COMPETING FINANCIAL INTERESTS The authors declare no competing financial interests.

[10]Division of Medical Oncology, University of Colorado Denver School of Medicine, Aurora, Colorado, USA.

[11]The Surgery Branch, National Cancer Institute, NIH, Bethesda, Maryland, USA.

Abstract

The incidence of melanoma is increasing more than any other cancer, and knowledge of its genetic alterations is limited. To systematically analyze such alterations, we performed whole-exome sequencing of 14 matched normal and metastatic tumor DNAs. Using stringent criteria, we identified 68 genes that appeared to be somatically mutated at elevated frequency, many of which are not known to be genetically altered in tumors. Most importantly, we discovered that *TRRAP* harbored a recurrent mutation that clustered in one position (p. Ser722Phe) in 6 out of 67 affected individuals (~4%), as well as a previously unidentified gene, *GRIN2A*, which was mutated in 33% of melanoma samples. The nature, pattern and functional evaluation of the *TRRAP* recurrent mutation suggest that *TRRAP* functions as an oncogene. Our study provides, to our knowledge, the most comprehensive map of genetic alterations in melanoma to date and suggests that the glutamate signaling pathway is involved in this disease.

Approximately 69,000 individuals were diagnosed with invasive melanoma in the United States in 2010, and there were approximately 8,700 deaths from melanoma in that year[1]. New insights into the pathogenesis of this lethal disease are needed. Although candidate gene analyses have been powerful in identifying melanoma mutations, such those in as *BRAF*, *cKit* and *ERBB4* (refs. 2–4), and whole-genome sequencing of a single melanoma has been completed[5], no comprehensive analysis of this tumor type has yet been performed. We have now used whole-exome sequencing to search for additional candidate melanoma genes in an unbiased fashion.

We conducted an exome resequencing of 14 matched normal and metastatic tumor DNAs from untreated individuals with melanoma. We enriched exonic sequences using Agilent's SureSelect technology for targeted exon capture[6], targeting 37 Mb of sequence from exons and their flanking regions in ~20,000 genes. We performed sequencing with the Illumina GAII platform and aligned the reads using ELAND (Illumina, Inc.) followed by cross_match (see URLs) to the reference human genome (build 36.1). On average, we generated 12 Gb of sequence per sample to a mean depth of 180× or greater to achieve exome builds with at least 90% of the exons covered by high quality genotype calls. To eliminate common germline mutations, we removed any potential somatic mutation that was observed in dbSNP130 or in the 1000 Genomes Project data. To determine which of these alterations were somatic (that is, tumor-specific), we compared these data to the matched normal tissue. From these putative alterations, we identified 5,161 potential somatic mutations in 3,568 different genes in the 14 samples sequenced.

To discriminate true mutations from the possible sequence alterations identified, we applied several steps, described in the **Supplementary Note** and **Supplementary Table 1**. These refinements gave us a 97.9% coverage rate, a 2.4% false-negative rate and a sensitivity of 81%. Furthermore, these tools removed ~18% of the alterations, leaving 4,226 putative somatic alterations for further scrutiny. A total of 3,871 alterations were heterozygous, and 355 changes were putative alterations in regions of loss of heterozygosity (**Supplementary Table 2**). Of these alterations, 2,813 caused amino acid changes (non-synonymous), including 2,589 missense and 175 nonsense alterations, and 49 occurred at splice sites. There were 1,387 silent (synonymous) substitutions. We observed a total of 18 small deletions and 9 insertions.

The observed somatic mutations could either be 'driver' mutations that have a role in melanoma neoplasia or functionally inert 'passenger' changes. This screen yielded a ratio of non-synonymous to synonymous changes (N:S ratio) of 2.0:1, which is not higher than the N:S ratio of 2.5:1 predicted for non-selected passenger mutations[7], suggesting that most of these alterations are likely to be 'passenger' mutations. The number of C>T mutations was significantly greater than the numbers of other nucleotide substitutions, resulting in a high prevalence of C>T/G>A transitions ($P < 0.001$) (**Supplementary Fig. 1**). Finally, we observed a total of 116 dinucleotide substitutions; of these, 59 were CC>TT/GG>AA changes, all consistent with the previously documented ultraviolet light exposure signature[8].

To search for new recurrent mutations, we looked for alterations that occurred in 2 or more of the 14 samples subjected to whole-exome sequencing. From this analysis, as expected, the BRAF p.Val600Glu alteration was captured in 7 out of the 14 samples. In addition to *BRAF*, we found nine more genes harboring a recurrent mutation. Seven of the new recurrent mutations were non-synonymous and two were synonymous (**Table 1**). Further screening of the new hotspot mutations in an additional 153 melanomas identified *DCC* and *ZNF831* to have a third recurring mutation each. Strikingly, *TRRAP*, encoding the transformation/transcription domain-associated protein, contained four additional cases that harbored the identical mutation (**Fig. 1** and **Supplementary Fig. 2**), one of which we found in the commercially available melanoma cell line A375. The recurring mutation in *TRRAP* was a cytosine to thymine change at position 2,165 of the transcript (uc003upp.1), leading to a serine to phenylalanine substitution at amino acid residue 722 of the protein (p.Ser722Phe). The likelihood for the occurrence of six identical mutations is approximately 5×10^{-20}, suggesting that the *TRRAP* hotspot mutation is important.

Subsequent sequence analysis of all coding exons of *TRRAP* in 25 additional melanomas revealed no additional non-synonymous alterations. The positions of the mutations in TRRAP imply that they are likely to be oncogenic, as we observed no truncating mutations, and 100% of the alterations occurred in one location. In addition, the affected residue is highly conserved evolutionarily (**Supplementary Fig. 3**). The clustering of somatic missense mutations is similar to that observed for activating mutations, such those in as *RAS* (ref. 9), *BRAF* (ref. 2) and *PIK3CA* (ref. 10), suggesting that *TRRAP* may be a new oncogene.

TRRAP functions as part of a multiprotein coactivator complex possessing histone acetyltranferase activity that is central to the transcriptional activity of p53, c-Myc and E2F1 (refs. 11,12). To determine whether the TRRAP recurrent alteration (p.Ser722Phe) is transforming, we transiently transfected NIH 3T3 cells with empty vector, wild-type TRRAP, mutant TRRAP or oncogenic Ras with p.Gly12Val. Two weeks after transfection, mutant TRRAP transformed NIH 3T3 cells more efficiently than wild-type TRRAP (**Fig. 2a**). Levels of TRRAP were comparable between the transfected cells (**Fig. 2b**).

To assess if melanoma cells harboring endogenous *TRRAP* mutations are dependent on *TRRAP* for survival, we used short hairpin RNA (shRNA) to stably knockdown TRRAP protein levels in melanoma cells harboring either wild-type *TRRAP* (SK-Mel-28 and 17T) or mutant *TRRAP* (63T and A375). We confirmed specific targeting of *TRRAP* by immunoblotting of transiently transfected HEK293T cells or one of the targeted melanoma cell lines (**Fig. 2c,d**). We grew clones in 10% or 2.5% serum to test cell viability. Knockdown of TRRAP had minimal effect on the survival of cells expressing wild-type *TRRAP* but substantially increased apoptosis rates of melanoma lines carrying mutant *TRRAP*, particularly when the clones were grown in low serum (**Fig. 2e–h** and **Supplementary Fig. 4**). These results were corroborated by protein blot analysis, which showed increased levels of cleaved PARP, specifically in mutant cells knocked down for

TRRAP as compared to vector control, as well as to TRRAP wild-type cells (**Fig. 2i,j**). Thus, mutant TRRAP is essential for melanoma cell survival, which is consistent with previous results showing that TRRAP knockout mice are embryonic lethal[13].

To further evaluate the prevalence and spectrum of somatic mutations in genes identified in the whole-exome discovery screen, we selected genes with more mutations than expected using the observed mutation rate (binomial $P < 0.05$; see Online Methods) (**Supplementary Table 3**) and those that were mutated in more than two discovery screen samples. We identified 16 such genes and analyzed them for mutations in an additional 38 melanoma samples using PCR amplification and Sanger sequencing. We identified a total of 65 putative changes in the prevalence screen (**Table 2**).

Notably, we found these sixteen genes, which, except for *BRAF*, had not previously been identified as playing a role in melanoma, to scale up and harbor an increasing number of somatic mutations in the prevalence screen. This correlated with the initial frequency identified in the discovery screen (**Table 2** and **Supplementary Table 4**). SIFT analysis predicted that a large fraction of the alterations would affect protein function (**Supplementary Table 5**).

We found *GRIN2A*, which was mutated in 6 of the 14 melanomas in the discovery screen, to harbor an additional 11 somatic mutations in the prevalence screen. In addition to the discovery and prevalence screen samples, we searched for *GRIN2A* somatic mutations in two independent validation panel sets from individuals with melanoma. Validation panel set 1, which included 39 melanomas, revealed 11 *GRIN2A* somatic mutations (28.2%), and validation panel set 2, which included 32 melanomas, identified 5 tumors with mutations (15.6%). Lastly, *GRIN2A* sequencing in 12 commercially available cell lines revealed a mutation in the 501Mel cell line. In total, we identified 34 distinct *GRIN2A* mutations in 135 samples (25.2%) (**Supplementary Table 4**). The number of C>T mutations identified in *GRIN2A* was significantly greater than the numbers of other nucleotide substitutions, resulting in a high prevalence of C>T/G>A transitions ($P < 0.001$) (**Supplementary Fig. 5**). **Supplementary Figure 6** depicts the various genetic and analytic stages used in our study.

GRIN2A, found on chromosome 16p13.2, encodes a glutamate (N-methyl-(D)-aspartic acid (NMDA)) receptor subunit ε-1 that is part of the class of ionotropic glutamate receptors and bears the agonist binding site for glutamate[14]. The location of the discovered GRIN2A alterations is summarized in **Figure 3**. We observed two mutation clusters surrounding amino acids 371, 372 and 373 in the PBP1 iGluR NMDA NR2 domain and 1,073, 1,074 and 1,076 in the NMDAR2 C domain. In addition, we observed three recurrent alterations (p.Ser278Phe, p.GluE371Lys and p.Glu1175Lys). The affected residues within these clusters are highly conserved evolutionarily, and SIFT analysis predicts that over 51% would affect protein function (**Supplementary Table 5**). Furthermore, we identified five nonsense mutations.

The nature of somatic mutations in tumors may aid in classifying the identified genes as oncogenes or tumor suppressors[15]. Generally, oncogenes harbor adjacent missense recurrent mutations that affect one allele. Tumor suppressor genes are generally mutated throughout the gene; many of the mutations truncate the protein and generally affect both alleles. Based on this classification, the mechanism by which mutations in *GRIN2A* have a tumorigenic effect is unclear; however, their frequency strongly suggests that they play a major role in melanoma and are worthy of future investigation.

The comprehensive approach to acquiring data in this study provided an opportunity to investigate whether any particular new gene pathways have a role in melanoma (Online Methods). From this analysis, we found the glutamate signaling pathway to be highly

significant. Glutamate is known to activate two different types of receptors: iono-tropic glutamate receptors (iGluRs) and metabotropic glutamate receptors (mGluRs). iGluRs are ligand-gated ion channels that allow cations such as calcium and potassium to pass through the plasma membrane of the cell after the binding of glutamate to the receptors. iGluRs are subdivided into three receptor types according to agonists response, one of which is *N*-methyl-D-aspartate (NMDA)[16]. Thus, *GRIN2A*, the most highly mutated gene in our screen, encodes a glutamate receptor subunit that binds NMDA. Another highly mutated gene identified was *PLCB4*, which encodes a downstream protein involved in metabotropic glutamate receptor-related signal transduction causing inositol phosphate production and protein kinase C (PKC) activation[17].

Importantly, a recent genetic analysis of the G-protein coupled receptor family in melanoma identified that GRM3, a metabotropic glutamate receptor also activated by glutamate, is mutated in 16% of melanoma cases (Prickett, T.D. *et al*., unpublished data). In this case as well, the GRM-signaling downstream effector PLCB4 is activated. Finally, a survey of the tyrosine kinome in melanoma has pointed to ERBB4, Pyk2 and the Ephrin receptors to be highly mutated[4]. Interestingly, ERBB4, its ligand NRG1, Pyk2 and the Ephrins have been shown to play a crucial role in modulation of NMDA receptor signaling[18–21]. Thus, molecular and genetic studies have implicated crosstalk between NRG1-ERBB4, GRM3, Ephrin signaling and glutamate receptor functions. A link between the glutamate pathway and tumorigenesis has been seen in neuronal tumors, where glioma cells releasing an excess of glutamate showed more aggressive growth than parental glioma cells[22]. Furthermore, previous reports showing that expression of GRM1 results in melanocytes transformation[23,24] also implicated glutamate signaling in melanoma. A glutamate pathway schematic summarizing these various components is depicted in **Supplementary Figure 7**.

Our study presents, to our knowledge, the most complete analysis of melanoma exome alterations to date, thus allowing us to (i) identify *TRRAP* as an unexpected target of recurring genetic alterations, (ii) reveal genes that were not previously connected with melanoma, one of which, *GRIN2A*, is one of the most highly mutated in melanoma to date and (iii) show that a majority of melanoma tumors had alterations in genes encoding members of the glutamate signaling pathway.

The results may enhance our biological insight of melanoma and will hopefully direct us toward new strategies to improve patient care. Some of our findings have potential therapeutic implications, as gluta-mate pathway modification has previously been shown to limit tumor growth[25]. Further investigation of this pathway in melanoma as well as development of such inhibitors is warranted.

METHODS

Methods and any associated references are available in the online version of the paper at http://www.nature.com/naturegenetics/.

Supplementary Material

Refer to Web version on PubMed Central for supplementary material.

Acknowledgments

We thank V. Maduro, H. Abaan, P. Cruz and J. Mullikin for generating the sequence data analyzed here. We thank V.G. Prieto for pathologic review of the biospecimens from MelCore at MD Anderson. We thank T. Wolfsberg for bioinformatics help and J. Fekecs and D. Leja for graphical assistance. This work was supported by the Intramural Research Programs of the National Human Genome Research Institute, the National Cancer Institute, National

Institutes of Health, USA and The University of Texas MD Anderson Cancer Center Melanoma SPORE (P50 CA93459).

ONLINE METHODS

Tumor tissues

Tissue and melanoma cell lines used for the discovery and prevalence screen in this study were described previously[26]. Tissues used for validation set 1 were fresh frozen melanoma tumors obtained from the University of Colorado Denver Skin Cancer Biorepository, Division of Medical Oncology. Tissue was collected at University of Colorado Hospital, Anschutz Medical Campus, under that institution's Institutional Review Board protocols. DNA was isolated from enriched macrodissected tumor isolates as previously described (see URLs). Tissue processing and storage procedures have been previously described[27]. Tissues used for validation set 2 of melanomas were obtained from optimum cutting temperature–embedded frozen clinical specimens from the Melanoma Informatics, Tissue Resource, and Pathology Core (MelCore) at The University of Texas MD Anderson Cancer Center under that institution's Institutional Review Board approved protocols. DNA isolation from the tumor-enriched isolates has been described previously[28]. The clinical information associated with the melanoma tumors used in this study is provided in **Supplementary Table 6**.

Exome capture

Exome capture was performed using the SureSelect Human All Exon System (Agilent Technologies). The manufacturer's protocol for SureSelect Human All Exon System (Illumina Paired-End Sequencing Library Prep), version 1.0.1 was used, with the following modifications: Bioanalyzer steps were either performed using agarose gel or omitted. In the sample preparation step 9, samples were purified using Ampure XP beads (Agencourt/Beckman Coulter Genomics) according to the manufacturer's protocols. In step 12, samples were purified with the QIAquick MinElute kit (Qiagen Inc.). One column was used for each sample; the four 250-μl post-amplification aliquots were pooled and passed over the column in several spin steps. Samples were eluted in 12 μl buffer EB and quantitated using the Qubit dsDNA BR Assay kit (Invitrogen Corp). In the post-hybridization amplification step 2, samples were purified with AMPure XP beads as described above. Samples were then eluted in 30 μL buffer EB.

Illumina sequencing

Sequencing was performed on the Illumina GAIIx platform with version 4 chemistry and version 4 flowcells according to the manufacturer's instructions. Seventy six base paired-end reads were generated.

Read mapping and variant analysis

Reads were initially aligned using ELAND (Illumina Inc.). ELAND alignments were used to place reads in bins of about five million base pairs. Unmapped reads were placed in the bin of the mate pair if the mate was mapped. Cross_match (P. Green, see URLs) was used to align the reads assigned to each bin to the corresponding ~5 Mb of genomic sequence. Cross_match alignments were converted to the SamTools bam format, and then genotypes were called using bam2mpg[29] (see URLs). Bam2mpg was used to implement the most probable Genotype (MPG) algorithm and a Bayesian based method was used to determine the probability of each genotype given the data observed at that position. The quality score represents the difference of the log likelihoods of the most and second most probable

genotype. The MPG was divided by the coverage at each position to calculate the MPG:coverage ratio.

To eliminate common germline mutations from consideration, alterations observed in dbSNP130 or in the 1000 Genomes Project 11_2010 data release project (see URLs) were removed. From this list of variants, we included those positions called by at least three of the four analysis methods used by the project. We further limited the list to those variants above 5% minor allele frequency. Polymorphisms were further removed by examination of the sequence of the gene in genomic DNA from matched normal tissue. Genotypes were annotated as described previously[30]. The types of mutation are: synonymous (changes protein coding region but not the amino acid), non-synonymous (changes protein coding region), missense variant (changes amino acid), nonsense variant, stop (introduces a stop codon), DIV-c (in-frame deletion or insertion variant in a coding region) and DIV-fs (frameshifting deletion or insertion variant in a coding region).

Statistical analysis of mutated genes

To determine which genes in the discovery screen were likely to be drivers, we calculated two metrics to assess the frequency and probability of mutations. The first method considered the frequency of mutations in the discovery screen, which was calculated by dividing the total number of non-synonymous mutations observed by the total number of base pairs sequenced. The second method fit a binomial distribution based on the number of base pairs sequenced for the gene of interest, the number of mutations observed and the background rate of mutation. For the background rate, we used the observed rate in the exome screen: 11.2 mutations per Mb. With this study design, our power to detect genes mutated in more than 20% of tumors was over 95%; using the two-mutation threshold, the detection probability was 80%.

PCR, sequencing and mutational analysis of melanoma samples

Genes identified to harbor recurrent mutations were confirmed, and further screened using two primer sets listed in **Supplementary Table 7** in an additional 153 melanoma samples. A subset of 16 genes found mutated in the discovery screen was selected for analysis in the prevalence screen using criteria described in the text. These genes were amplified and sequenced in an additional 38 melanoma samples using the primers listed in **Supplementary Tables 7** and **8**. BRAF was only evaluated for the V600E alteration. Mutational analysis, confirmation and determination of somatic status were carried out as previously described[4,26]. All genes had 93% coverage or above.

Plasmid cloning

TRRAP expressing construct in the CβSBS vector was a kind gift from M. Cole (Norris Cotton Cancer Center Lebanon, New Hampshire, USA). The TRRAP mutation was generated as previously described[26] using primers shown in **Supplementary Table 9**. The TRRAP mutation bearing the PCR product was inserted in the TRRAP-CβSBS plasmid. Sequence-verified mutant TRRAP was subsequently used in the various experiments. Details are available upon request.

Cell culture and transient expression

Metastatic melanoma tumor lines were maintained as previously described[26]. HEK 293T cells were purchased from American Type Culture Collection (ATCC), and SK-Mel-28 and A375 cells were purchased from National Cancer Institute, Division of Cancer Treatment,

Developmental Therapeutics Program, Frederick, Maryland, USA. Cell lines were maintained as previously described[26].

Protein blotting

Transfected cells or stable clones were lysed as described[4]. Briefly sonicated whole cell extracts in 2×SDS sample buffer were subjected to protein blotting. Primary antibodies used were TRRAP antibody (Cell Signaling, Cat. No. 3966S), PARP antibody (Cell Signaling, Cat. No. 9542) and α-tubulin antibody (Calbiochem-EMD Biosciences, Cat. No. 555627).

Lentiviral shRNA

Constructs for stable depletion of TRRAP (Catalog# RHS4533, Construct# TRCN0000005361, TRCN0000005362) (Open Biosystems) were confirmed to knockdown TRRAP at the protein level. Lentiviral stocks were prepared as previously described[4]. Melanoma cell lines (63T, 17T, A375 and SK-Mel-28) were infected with control and TRRAP-specific shRNA lentiviruses. Selection and growth were done as previously described[26].

Apoptosis measurement

Cells were collected by incubation in trypsin containing EDTA followed by centrifugation and were fixed in a solution containing 3.7% formaldehyde, 0.5% NP40 and 10 μg/ml Hoechst 33258 in PBS. Apoptotic indices were determined by visual scoring of at least 300 nuclei.

NIH 3T3 transformation assay

For each plasmid (CβSBS, CβSBS -TRRAP (wild type), CβSBS -TRRAP (p.Ser722Phe) and Ras p.Gly12Val), 3 μg of plasmid was transfected using the calcium phosphate precipitation method into NIH 3T3 cells cultured in T25 flasks. Twenty-four hours after transfection, 1–5% of transfected cells were seeded into T25 flasks and cultured in growth medium containing 2.5% FBS for 14–20 days. The flasks were scored under a microscope by visually counting foci.

Pathway analysis

Three sources of gene sets were selected: Gene Ontology, Kyoto Encyclopedia of Genes and Genomes, and MSigDB (see URLs), containing 10,147, 214 and 1,892 groups, respectively, when downloaded in September 2010. The sets included groups based on molecular function, cellular localization, biological processes and signaling pathways. For each of group of genes, we examined whether we assessed the respective genes in the exome analysis and whether mutations were observed. Several different statistics were then calculated to accentuate different aspects of the analysis. First, we examined the number of genes we successfully sequenced in the study compared to the number that were mutated. This proportion was then compared to the background rate of 3,308 genes mutated in the total of 16,768 genes using a hypergeometric distribution. As the purpose was for ranking, no multiple comparison correction was implemented. Second, we examined the average number of non-synonymous mutations observed for the mutated genes by dividing the total number of non-synonymous mutations into the total number of genes observed to be mutated. Third, we used a binomial calculation. For each group of genes, we determined the total number of mutations observed and the number of base pairs that were successfully sequenced. We then computed the *P* value as the probability of a group having at least as

many mutations as were observed, given the numbers of base pairs sequenced and the background passenger frequencies, using the binomial distribution in R (see URLs). The background passenger frequencies were conservatively estimated as the total numbers of mutations observed the whole exome study divided by the total number of base pairs sequenced in the study (assuming that all of the mutations observed were passengers).

References

1. Jemal A, Siegel R, Xu J, Ward E. Cancer statistics, 2010. CA Cancer J. Clin. 2010; 60:277–300. [PubMed: 20610543]
2. Davies H, et al. Mutations of the *BRAF* gene in human cancer. Nature. 2002; 417:949–954. [PubMed: 12068308]
3. Curtin JA, Busam K, Pinkel D, Bastian BC. Somatic activation of KIT in distinct subtypes of melanoma. J. Clin. Oncol. 2006; 24:4340–4346. [PubMed: 16908931]
4. Prickett TD, et al. Analysis of the tyrosine kinome in melanoma reveals recurrent mutations in *ERBB4*. Nat. Genet. 2009; 41:1127–1132. [PubMed: 19718025]
5. Pleasance ED, et al. A comprehensive catalogue of somatic mutations from a human cancer genome. Nature. 2010; 463:191–196. [PubMed: 20016485]
6. Gnirke A, et al. Solution hybrid selection with ultra-long oligonucleotides for massively parallel targeted sequencing. Nat. Biotechnol. 2009; 27:182–189. [PubMed: 19182786]
7. Sjöblom T, et al. The consensus coding sequences of human breast and colorectal cancers. Science. 2006; 314:268–274. [PubMed: 16959974]
8. Greenman C, et al. Patterns of somatic mutation in human cancer genomes. Nature. 2007; 446:153–158. [PubMed: 17344846]
9. Bos JL, et al. Prevalence of *ras* gene mutations in human colorectal cancers. Nature. 1987; 327:293–297. [PubMed: 3587348]
10. Samuels Y, et al. High frequency of mutations of the *PIK3CA* gene in human cancers. Science. 2004; 304:554. [PubMed: 15016963]
11. McMahon SB, Van Buskirk HA, Dugan KA, Copeland TD, Cole MD. The novel ATM-related protein TRRAP is an essential cofactor for the c-Myc and E2F oncoproteins. Cell. 1998; 94:363–374. [PubMed: 9708738]
12. Barlev NA, et al. Acetylation of p53 activates transcription through recruitment of coactivators/histone acetyltransferases. Mol. Cell. 2001; 8:1243–1254. [PubMed: 11779500]
13. Herceg Z, et al. Disruption of Trrap causes early embryonic lethality and defects in cell cycle progression. Nat. Genet. 2001; 29:206–211. [PubMed: 11544477]
14. Johnson JW, Ascher P. Glycine potentiates the NMDA response in cultured mouse brain neurons. Nature. 1987; 325:529–531. [PubMed: 2433595]
15. Vogelstein B, Kinzler KW. Cancer genes and the pathways they control. Nat. Med. 2004; 10:789–799. [PubMed: 15286780]
16. Hollmann M, Heinemann S. Cloned glutamate receptors. Annu. Rev. Neurosci. 1994; 17:31–108. [PubMed: 8210177]
17. Pin JP, Gomeza J, Joly C, Bockaert J. The metabotropic glutamate receptors: their second intracellular loop plays a critical role in the G-protein coupling specificity. Biochem. Soc. Trans. 1995; 23:91–96. [PubMed: 7758811]
18. Anton ES, et al. Receptor tyrosine kinase ErbB4 modulates neuroblast migration and placement in the adult forebrain. Nat. Neurosci. 2004; 7:1319–1328. [PubMed: 15543145]
19. Rieff HI, et al. Neuregulin induces GABA(A) receptor subunit expression and neurite outgrowth in cerebellar granule cells. J. Neurosci. 1999; 19:10757–10766. [PubMed: 10594059]
20. Ozaki M, Sasner M, Yano R, Lu HS, Buonanno A. Neuregulin-β induces expression of an NMDA-receptor subunit. Nature. 1997; 390:691–694. [PubMed: 9414162]
21. Dalva MB, et al. EphB receptors interact with NMDA receptors and regulate excitatory synapse formation. Cell. 2000; 103:945–956. [PubMed: 11136979]

22. Takano T, et al. Glutamate release promotes growth of malignant gliomas. Nat. Med. 2001; 7:1010–1015. [PubMed: 11533703]
23. Pollock PM, et al. Melanoma mouse model implicates metabotropic glutamate signaling in melanocytic neoplasia. Nat. Genet. 2003; 34:108–112. [PubMed: 12704387]
24. Shin SS, et al. Oncogenic activities of metabotropic glutamate receptor 1 (Grm1) in melanocyte transformation. Pigment Cell Melanoma Res. 2008; 21:368–378. [PubMed: 18435704]
25. Rzeski W, Turski L, Ikonomidou C. Glutamate antagonists limit tumor growth. Proc. Natl. Acad. Sci. USA. 2001; 98:6372–6377. [PubMed: 11331750]
26. Palavalli LH, et al. Analysis of the matrix metalloproteinase family reveals that MMP8 is often mutated in melanoma. Nat. Genet. 2009; 41:518–520. [PubMed: 19330028]
27. Morente MM, et al. TuBaFrost 2: standardising tissue collection and quality control procedures for a European virtual frozen tissue bank network. Eur. J. Cancer. 2006; 42:2684–2691. [PubMed: 17027255]
28. Davies MA, et al. Integrated molecular and clinical analysis of AKT activation in metastatic melanoma. Clin. Cancer Res. 2009; 15:7538–7546. [PubMed: 19996208]
29. Teer JK, et al. Systematic comparison of three genomic enrichment methods for massively parallel DNA sequencing. Genome Res. 2010; 20:1420–1431. [PubMed: 20810667]
30. Biesecker LG, et al. The ClinSeq Project: piloting large-scale genome sequencing for research in genomic medicine. Genome Res. 2009; 19:1665–1674. [PubMed: 19602640]

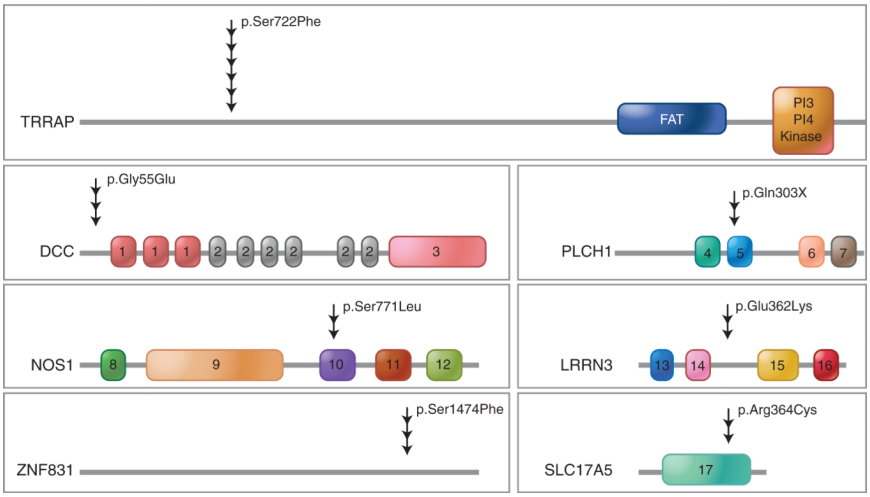

Figure 1.

Distribution of new non-synonymous recurrent mutations. Seven new non-synonymous recurrent mutations identified in this study are presented on relevant protein schematics. Black arrows indicate locations of recurrent mutations and conserved protein functional domains are indicated as colored boxes (1, immunoglobulin I-set domain; 2, fibronectin type III domain; 3, neogenin C terminus; 4, phosphoinositide-specific phospholipase C, efhand-like; 5, phosphatidylinositol-specific phospholipase C, X domain; 6, phosphatidylinositol-specific phospholipase C, Y domain; 7, C2 domain; 8, PDZ domain; 9, nitric oxide synthase, oxygenase domain; 10, flavodoxin; 11, FAD binding domain; 12, oxidoreductase NAD-binding domain; 13, LRRNT, leucine rich repeat N-terminal domain; 14, leucine rich repeat; 15, immunoglobulin I-set domain; 16, fibronectin type III domain; 17, major facilitator superfamily).

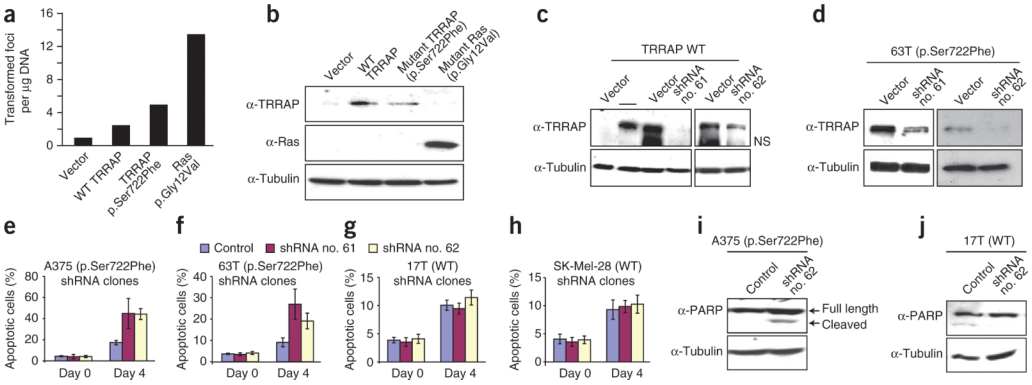

Figure 2.

Effect of mutant TRRAP on colony formation and apoptosis. (**a**) Mutant TRRAP induces cell transformation. Foci formation of NIH 3T3 cells transfected with the indicated constructs or empty vector control. Ras p.Gly12Val was included as a positive control for cell transformation. (**b**) Detection of TRRAP and KRas protein expression in lysates of transiently transfected NIH 3T3 cells by immunoblot analysis. (**c**) Immunoblot of cell lysates from HEK 293T cells transiently transfected with either control vector or shRNAs that target TRRAP. For normalization, lysates were analyzed in parallel by anti–α-tubulin immunoblotting. NS, non specific. (**d**) Immunoblot of melanoma cells transduced with shRNA targeting TRRAP and immunoblotted with anti-TRRAP. (**e–h**) TRRAP mutation confers resistance to apoptosis. Apoptosis quantification of melanoma cell lines transduced with shRNA control or shRNAs targeting TRRAP by Hoechst 33258-staining. Cells were grown in growth medium containing 2.5% serum for the indicated times. Error bars, s.d. (**i,j**) Immunoblot analysis of representative melanoma lines presented in **e–h** using the indicated antibodies to assess PARP cleavage. WT, wild type.

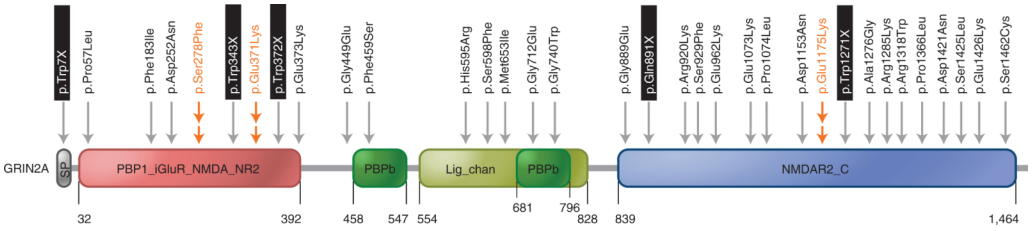

Figure 3.

Location of somatic mutations in GRIN2A. A schematic of human GRIN2A is presented, with conserved functional domains indicated as colored blocks. Somatic mutations are indicated with arrows and amino acid changes. Recurrent mutations and nonsense mutations are indicated as orange arrows and black boxes, respectively. Conserved domains: SP, signal peptide; PBP1_iGluR_NMDA_NR2, N-terminal leucine/isoleucine/valine-binding protein LIVBP-like domain of the NR2 subunit of NMDA receptor family; PBPb, bacterial periplasmic substrate-binding protein; Lig_chan, ligand-gated ion channel; NMDAR2_C, N-methyl D-aspartate receptor 2B3 C terminus.

Table 1

Recurrent mutations identified in melanoma whole exome sequencing and prevalence screen

Gene name	# of tumors affected	Nucleotide change	Amino acid change	Synonymous or non-synonymous	Tumor name	Tumor panel
BRAF	7	c.1799T>A	p.Val600Glu	Non-synonymous	1T	Exome capture
					5T	Exome capture
					9T	Exome capture
					22T	Exome capture
					35T	Exome capture
					51T	Exome capture
					91T	Exome capture
CPT1A	2	c.1638C>T	p.Phe546Phe	Synonymous	5T	Exome capture
					43T	Exome capture
DCC	3	c.164G>A	p.Gly55Glu	Non-synonymous	12T	Exome capture
					18T	Exome capture
					MB1160_T	Validation set 1
FCRL1	3	c.741C>T	p.Ile247Ile	Synonymous	91T	Exome capture
					96T	Exome capture
					63T	Prevalence screen
LRRN3	2	c.1084G>A	p.Glu362Lys	Non-synonymous	12T	Exome capture
					24T	Exome capture
NOS1	2	c.2312C>T	p.Ser771Leu	Non-synonymous	24T	Exome capture
					60T	Exome capture
PLCH1	2	c.907C>T	p.Gln303X	Non-synonymous	1T	Exome capture
					24T	Exome capture
SLC17A5	2	c.1090C>T	p.Arg364Cys	Non-synonymous	12T	Exome capture
					18T	Exome capture
TRRAP	6	c.2165C>T	p.Ser722Phe	Non-synonymous	63T	Exome capture
					91T	Exome capture
					96T	Prevalence screen
					106T	Prevalence screen
					119T	Prevalence screen
					A375	Commercial cell line

Gene name	# of tumors affected	Nucleotide change	Amino acid change	Synonymous or non-synonymous	Tumor name	Tumor panel
ZNF831	3	c.4421C>T	p.Ser1474Phe	Non-synonymous	43T	Exome capture
					91T	Exome capture
					MB1160_T	Validation set 1

Samples used in the exome capture and prevalance screen were obtained from the Surgery Branch, National Cancer Institute. Validation set 1 samples were obtained from The Division of Medical Oncology, University of Colorado Denver School of Medicine. A375 is a commercially available melanoma cell line. Listed *BRAF* mutations are from the whole-exome study only. Based on genome build hg18 (NCBI 36.1). Number of samples investigated: exome capture, $n = 14$; prevalence screen, $n = 70$; validation set 1, $n = 39$; validation set 2, $n = 32$; commercial cell lines, $n = 12$.

Table 2

Whole exome sequencing in melanoma revealed sixteen highly mutated genes

			Exome capture (n = 14)			Prevalence screen (n = 38)			Combined exome capture and prevalence screen (n = 52)		
Gene name	**UCSC ID**	***P***	**No. of non-synonymous mutations**	**No. of tumors affected**	**% of tumors affected**	**No. of non-synonymous mutations**	**No. of tumors affected**	**% of tumors affected**	**No. of non-synonymous mutations**	**No. of tumors affected**	**% of tumors affected**
BRAF	uc003vwc.2	4.80×10^{-5}	7	7	50.0	27	27	71.1	34	34	65.4
GRIN2A	uc002czq.1	6.36×10^{-3}	6	6	42.9	11	11	28.9	17	17	32.7
CCDC63	uc001trv.1	3.34×10^{-3}	4	4	28.6	2	2	5.3	6	6	11.5
TMEM132B	uc001uhe.1	7.59×10^{-3}	5	4	28.6	5	5	13.2	10	9	17.3
ZNF831	uc002yan.1	1.29×10^{-2}	5	4	28.6	5	5	13.2	10	9	17.3
PLCB4	uc010gbx.1	4.39×10^{-2}	4	4	28.6	4	4	10.5	8	8	15.4
AKR1B10	uc003vrr.1	5.21×10^{-3}	3	3	21.4	1	1	2.6	4	4	7.7
TAS2R60	uc003wdb.1	5.46×10^{-3}	3	3	21.4	2	2	5.3	5	5	9.6
KHDRBS2	uc003peg.2	7.26×10^{-3}	3	3	21.4	2	2	5.3	5	5	9.6
PTPRO	uc001rda.1	9.09×10^{-3}	3	3	21.4	1	1	2.6	4	4	7.7
SYT4	uc002law.1	1.23×10^{-2}	3	3	21.4	1	1	2.6	4	4	7.7
UGT2B10	uc003hee.1	2.13×10^{-2}	3	3	21.4	1	1	2.6	4	4	7.7
SLC6A11	uc003bvz.1	2.84×10^{-2}	3	3	21.4	0	0	0.0	3	3	5.8
SLC17A5	uc003phn.2	7.91×10^{-3}	4	3	21.4	0	0	0.0	4	3	5.8
C12orf63	uc001tet.1	4.46×10^{-2}	4	3	21.4	2	2	5.3	6	5	9.6
PCDHB8	uc003liu.1	4.80×10^{-2}	3	3	21.4	1	1	2.6	4	4	7.7

Based on genome build hg 18 (NCBI 36.1).